10
A Reductionist Approach to Creating and Using Neuromusculoskeletal Models

Ian E. Brown and Gerald E. Loeb

1 Introduction

There are many possible approaches for developing models of physical systems. At one extreme exists the black-box model in which only the inputs and outputs of the system are considered important aspects of the model (see Chapter 9). Alternatively one can divide a system into separate components and model each component separately (see Chapter 8). The most obvious difference between these approaches is that there is more information in the latter model than just the inputs and outputs of the system. This latter approach is loosely termed reductionism—the form of the model for the system is 'reduced' into smaller components, each of which should have some testable relationship to a corresponding physical structure.

For the beginner modeler who is exploring various avenues of model development, the key question is which approach to use? The short answer is that the optimal approach will depend upon the desired use of the model. If all that is of concern are the inputs and outputs of the system, then the black-box approach (which is often easiest) is probably the most logical. On the other hand, if there is a desire to understand the relative importance of various internal components or to associate various emergent properties of the whole system with one or more of the internal components, then the reductionist approach has an obvious advantage. Furthermore, models often need to be extrapolated to predict outputs under conditions that lie outside those for which black-box data are available; reductionist models may be more robust in such applications.

There are two other potential advantages to using reductionist models. First, it is easier to design experiments for and to model small, simple components from a reduced system, than it is for large, complex systems. Second, reductionist models can often be produced more easily than black-box models when the goal is to create models of many similar systems. For example, consider two systems that are similar but not identical. The black-box approach would have to be fully validated twice, once for each system. Conversely, the reductionist approach would only need to revise the models for those components that are not identical.

Because this book is about neuromusculoskeletal (NMS) systems, the rest of this chapter will focus upon modeling the NMS system. We believe that the reductionist approach is useful for modeling this system for the reasons supplied above; the model that is presented here is in the form of a reductionist model. To demonstrate the advantages of this approach, published examples of observations that were understood or explained with the help of a reductionist model will be given. The chapter will then end with a detailed example of a previously unpublished study that could only be undertaken with the use of a reductionist model.

2 Reduction to Practice

The neuromusculoskeletal (NMS) system is particularly well suited for reductionist modeling. A simple examination of the NMS apparatus reveals several distinct types of components that occur more often than once. Although the individual compo-

Brown, I.E. and Loeb, G.E. A reductionist approach to creating and using neuromusculoskeletal models. Chapter in: *Biomechanics and Neuro-Control of Posture and Movement*, (Eds.) J. Winters and P. Crago, Springer-Verlag, New York, 2000, pp 148-163.

nents within various NMS systems may be similar, the relative numbers and proportions of these components may vary. Black-box modeling would require independent models for each and every system, whereas a well-designed reductionist model could reuse components from one model to the next.

A key issue in reductionist models is how much to reduce the system. For example, there are many useful approaches for reducing muscle: one can break it into tendon and fascicle; tendon, aponeurosis, and fascicle, or even a population of collagen fibers for each of tendon and aponeurosis and a population of cross-bridges, z-lines and myofilaments for each of the fibers within each fascicle. To resolve the issue of how much to reduce a system requires a precise goal (i.e., different studies with different goals will produce or use different degrees of reduction).

The model that we use and are continuing to build is based on the following goal: to be able to correctly predict for any NMS system operating under physiological conditions the resultant kinematics and kinetics for a given neural input and to be able to associate various emergent properties of the NMS system with specific anatomical structures. This is a rather lofty goal that is pursued by many laboratories, but by defining it for ourselves, the appropriate structure for our model becomes clearer.

Given the previously stated goal for our NMS model, it is obvious that we must use a reductionist approach for our design. By choosing components that are common to various NMS systems and modeling these components individually, every time that we are interested in a new NMS system, we are not required to start from the beginning. The question remains: how far do we keep reducing? The other consideration that helps define the answer to this question is the complexity of the model. If reducing a model offers no further insight (in the context of the stated goal) but increases the complexity, then it is not a useful step to take. Similarly, if reducing a given model further provides a marginal improvement of accuracy but a substantial increase in complexity, then it, too, is not a useful step to make.

As an example, the tendon is described as one component and is not modeled as a population of collagen fibers. A single component describing tendon as a nonlinear spring is far simpler then a population of collagen fibers, each of which is has its own complex properties. Introducing the population of collagen fibers does not produce any insight into how the whole system behaves under various conditions. On the other hand, researchers interested in understanding a nonlinear behaviour known to exist in the tendon (e.g., rupture) may want to model the tendon as a population of collagen fibers.

We divide our NMS model into three obvious subsystems: neural, muscular and skeletal (see Chapter 8 for a similar division into subsystems, and description of subsystem properties). Each of these large subsystems is then subdivided into useful smaller components. We provide examples from published studies to help demonstrate the usefulness of dividing the system as we have done.

2.1 The Skeletal System

The skeletal system refers to the skeleton itself. Physically this includes the bones and the joints connecting the bones. The mass associated with muscles, skin and other soft tissues has traditionally been lumped with the skeletal segments when analyzing NMS kinetics, although this may cause computational instabilities (He et al. 1991 and below) or even inaccuracies (Cavagna 1970). Because the forces produced by the muscular system act upon the skeletal system to produce torques around the various joints, the NMS model typically includes sufficient information about the position of the muscles and tendons to permit computation of muscle moment arms.

The components that we have chosen to use are linked segments and moment arms (see Figure 10.1). Mechanical segments are not necessarily identical to individual bones. For example, the shank (which includes two bones: the tibia and the fibula) could be considered a single segment. To be able to model external rotation of a single segment shank (which realistically entails a joint between the tibia and fibula) a rotational degree of freedom can be assigned to the knee itself without introducing significant error into the kinematics of muscles attaching on those bones. Segments have a length, a mass (and associated inertia) and are linked to other segments by joints with restricted

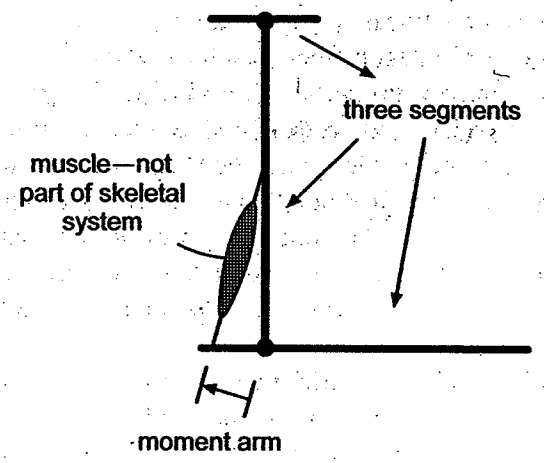

FIGURE 10.1. A sample musculoskeletal model of the arm to demonstrate the model components of the skeletal system. There are three segments and one moment arm in this example skeletal system.

degrees of freedom and ranges of motion. The choice of linkage usually reflects the purpose of the model as will be demonstrated in example A1. Conversely, moment arms are usually determined from the actual anatomy of the origin, insertion and tendon paths of muscles. As will be seen in example A2, however, it may be important, more efficient and more accurate to infer moment arms from kinematics instead of gross anatomy.

2.1.1 Example A1: Using an Appropriate Number of Segments

This example (from Zajac and Gordon 1989) compares two models of the body. The first model uses two segments to describe the body while the second model uses three segments. The question being asked was: what effect does activating soleus muscle (usually classified as an ankle extensor) have on the skeletal system?

If the body is modeled as two segments (Figure 10.2A), one for the foot and the other for the rest of the body, the equation relating angular acceleration around the ankle and net torque is:

$$\ddot{\theta} = \left(\frac{1}{\tilde{I}}\right) T^{NET} \tag{10.1}$$

Clearly, when soleus is activated in this model (increasing the net torque), it extends the ankle joint.

If the body is modeled as three segments (Figure 10.2B), foot, shank, and rest of body, then the equations become more complex (for a complete derivation, see Zajac and Gordon, [1989]):

$$\ddot{\theta}_1 = \frac{1}{\beta}\left\{\left[\frac{1}{\tilde{I}_1}\right] T_1^{NET} - \left[\frac{\tilde{I}_{CS}\cos(\theta_1 - \theta_2)}{\tilde{I}_1\tilde{I}_2}\right] T_2^{NET}\right\} \tag{10.2}$$

$$\ddot{\theta}_2 = \frac{1}{\beta}\left\{\left[\frac{1}{\tilde{I}_2}\right] T_2^{NET} - \left[\frac{\tilde{I}_{CS}\cos(\theta_1 - \theta_2)}{\tilde{I}_1\tilde{I}_2}\right] T_1^{NET}\right\} \tag{10.3}$$

where

$$\beta = [\tilde{I}_1\tilde{I}_2 - \tilde{I}_{CS}^2\cos^2(\theta_1 - \theta_2)]/(\tilde{I}_1\tilde{I}) > 0 \quad \text{for all } (\theta_1 - \theta_2)$$

Although these equations are not trivial, they clearly show that both of the angular accelerations (knee and ankle) are dependent upon both of the net torques (about the knee and ankle). In particular, if soleus is activated to produce a torque around the ankle, this will cause extension in the ankle AND extension in the knee. The significance of these results is that a muscle that was typically clas-

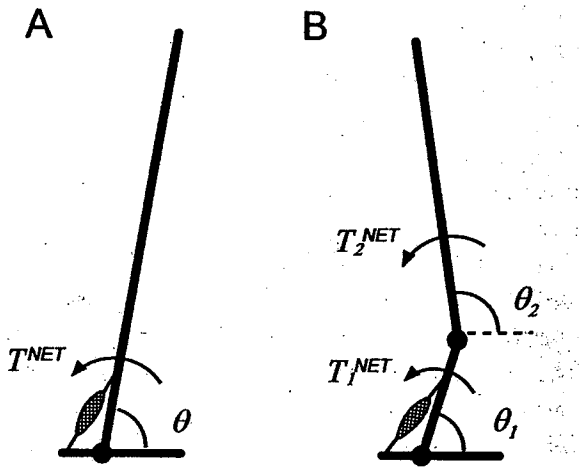

FIGURE 10.2. (A) A two-segment model of the body including the soleus muscle—one segment for the foot and the other segment for body. (B) A three-segment model of the body including the soleus muscle—one segment for the foot, one for the shank and one for the rest of the body. In both cases, each segment has a mass and associated inertia I. The net torques (T) are calculated from the torque due to soleus activation and the torque due to gravity. I_1 and I_2 refer to the inertias of the shank and body, respectively.

sified as an ankle extensor (because it only crosses the ankle joint), was shown to be able to produce knee extension in a particular circumstance. Only by incorporating an appropriate number of segments in the model was it possible to understand the system properly and consider more fully the possible implications of activating a particular muscle.

2.1.2 *Example A2: Changing Moment Arms*

When considering the role of a muscle, physiologists look at the muscle's moment arm and electromyogram (EMG) pattern during normal usage. Often the complexities of moment arm are not well understood or well modeled. The following example (from Young et al. 1993) shows how looking at muscle moment arms in three dimensions versus two dimensions can reveal large, previously unknown effects. The study by Young et al. (1993) also demonstrated that it is important to examine the full range of moment arms that a muscle might experience at different joint angles.

Eleven muscles that cross the ankle joint of the cat were examined by measuring length changes in response to angular motion of the ankle joint in all three planes. Most of these muscles have been classified according to their action in the parasagittal plane alone; the moment arms in the other planes were examined to see if this classification was appropriate. The results demonstrated that some of the muscles previously classified as ankle flexors/extensors had larger moment arms in the adduction/abduction axis (see Figure 10.3). The study went further to look at joint angle effects on moment arm and discovered that some moment arms changed dramatically with joint angle (see Figure 10.3, abduction/adduction moment arm). These results are significant because they alter our understanding of what these muscles can actually do. Such "details" have been discovered to correlate with the natural patterns of recruitment of the muscles (Abraham and Loeb 1985; Loeb 1993) and with their patterns of spinal reflex connectivity (Bonasera and Nichols 1996).

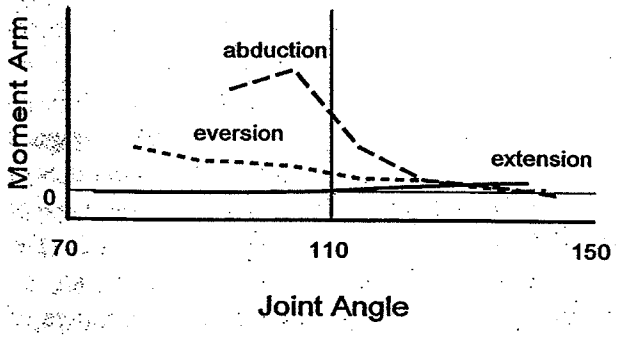

FIGURE 10.3. Moment arm versus joint angle relationship for peronius brevius. (Data originally published in Young et al. 1993.) The moment arms for the three different axes are plotted on the same figure for various joint angles (extension/flexion.)

Muscles that have a larger moment arm in nonparasagittal planes may be used for ankle flexion/extension, but cannot do so alone as their activation will also produce moments in other axes. Their primary usage may, in fact, not be as a flexor/extensor, but rather as an adductor/abductor. Furthermore, if a muscle has a very small moment arm when the ankle is in a neutral position, then the muscle is not particularly useful in moving the ankle out of neutral position. However, if the moment arm becomes larger as the joint angle moves away from the neutral position (as occurs for many of these ankle muscles), then the muscle can become very useful for returning the joint to neutral position (see Figure 10.4). Thus a muscle classified as an adductor may only be able to adduct so as long as the ankle is abducted. It may not be able to adduct the joint when it is in the neutral position or partially adducted. Only by examining the mo-

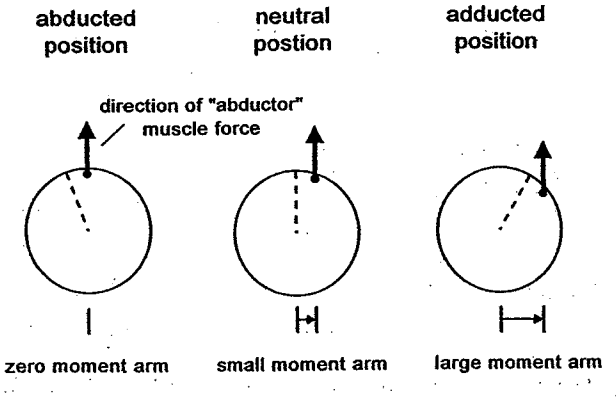

FIGURE 10.4. A schematic caudal view of the ankle with an "abductor" muscle. As the abduction/adduction angle changes (indicated by dashed lines), the moment arm produced by the muscle changes. While in the adducted position, the muscle has a large moment arm and would be a strong abductor. But as the angle changes towards abduction, the ability of the muscle to abduct decreases until the moment arm becomes zero.

ment arms thoroughly and individually can the potential usefulness of various muscles for certain tasks be understood.

2.2 The Muscular System

The muscular system includes individual muscles composed of tendon, aponeurosis and fascicles (bundles of fibers) as shown in Figure 10.5A. The major division into components for our model is along these anatomical lines as connective tissue and contractile tissue.

Connective tissue includes both the tendon and aponeurosis. These two tissues have nonlinear spring-like properties that are similar to each other (Scott and Loeb 1995). Because their properties are nearly identical, the two anatomically separate tissues are grouped together into a single component (series elastic element, SE in Figure 10.5B). The fascicles are classified as contractile tissue. It is generally assumed for simplicity that fibers within a muscle are identical and act together so that a single component (the fascicles) may be used to represent them. However, there are often different populations of fiber types within a muscle. In these cases, separate fascicles with different properties representing the populations of fibers may be used in parallel with each other. The fascicles in a real muscle may actually consist of shorter muscle fibers in series as well as in parallel (Loeb et al. 1987); this may be important for issues of mechanical stability (Loeb and Richmond 1994) but can be ignored for most normal behaviors by using the physiological cross-sectional area of the muscle instead of the morphometry of individual muscle fibers.

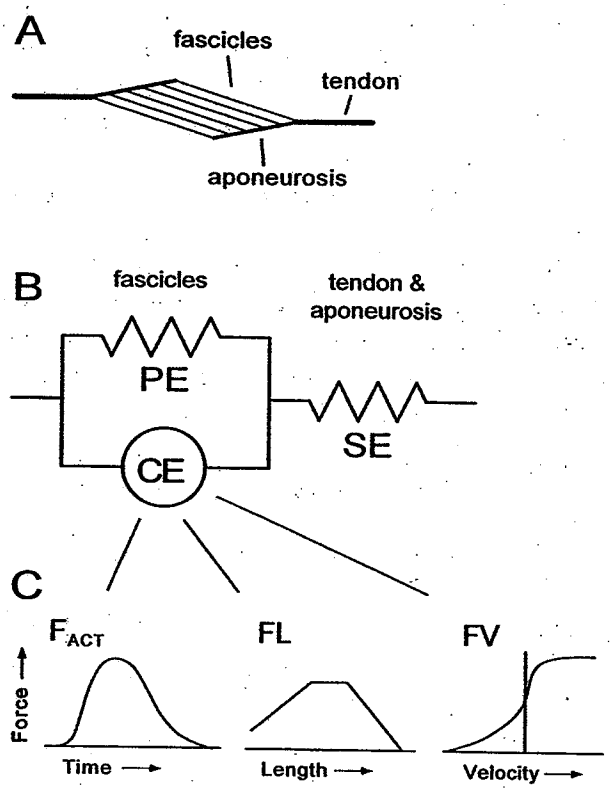

FIGURE 10.5. (A) Schematic figure of a typical muscle including the tendon, aponeurosis and fascicles. (B) Model components representing the muscle. The tendon and aponeurosis are combined to form the series elasticity (SE), while the fascicles are composed of the parallel elasticity (PE) and the contractile element (CE). (C) The CE can be subdivided into three components: activation (F_{ACT}), the force-length relationship (FL) and the force-velocity relationship (FV).

The fascicles themselves can be broken into two smaller mechanical subcomponents (Figure 10.5B)—the passive elastic element (PE) and the active contractile element (CE). In the passive state (no neural activation) fascicles behave much like a nonlinear spring. This property can be modeled and included as a passive component of the fascicles. When fascicles are activated neurally, they produce (active) force in parallel with and adding to the passive force.

The active component can be divided even further into three smaller subcomponents (Figure 10.5C; see also Chapters 7, 8, 11, 28, 43). The force-length (FL) component arises because of the change in actin/myosin overlap as the length of fascicles (and hence sarcomeres) changes. As the overlap between the myofilaments changes, the number of cross-bridge sites available for force generation changes (see Chapter 2). The force-velocity (FV) component is thought to arise because of cross-bridge dynamics (Huxley 1957). As muscles change length, cross-bridges complete their cycles, detach and reattach. The dynamics of attachment and detachment thus effect the shape of the FV relationship (see review in Chapter 2). The activation component (F_{ACT}) is associated with calcium kinetics. F_{ACT} represents the percentage of myosin binding sites on the thin filament that are available for cross-bridge formation, which depends upon sarcoplasmic calcium concentration. F_{ACT} thus consists of a function of time that relates motoneuron activity to calcium release and re-

uptake by the sarcoplasmic reticulum as well as sarcoplasmic calcium concentrations to myosin binding site availability.

The active component is divided in such a manner because historically it was observed that active force was affected by length, velocity and activation. The simplest approach to understanding these phenomena is thus to assume that they are independent and examine them one by one (i.e., hold two of them constant while varying one and measuring force). It has been through subsequent experiments that the underlying determinants for each of these factors were understood.

At this point, we should remind the readers of our goal: to be able to correctly predict for any NMS system under physiological conditions the resultant kinematics and kinetics for a given neural input and to be able to associate various emergent properties with anatomical structures. We are not interested in the biochemistry or molecular energetics involved in muscular contraction. Although those are both fascinating subjects, they require different models than the one presented here. Developing and testing theories about molecular energetics also may lead the experimenter to apply conditions of activation or kinematics that are unphysiological, such as tetanic stimulation or small, abrupt length changes. Models that account for the effects observed under such conditions may be excessively complex or unreliable when extrapolated to physiological conditions of muscle work. The following examples will address each of the levels of division that are used in our model

2.2.1 *Example B1: Separating the Contractile Tissue from the Connective Tissue*

As stated earlier, reducing a system increases the number of components and so tends to increase the complexity of the resultant model. However, not reducing a system sufficiently can result in difficulties in modeling the system accurately. Whether to separate the aponeurosis from the fascicles has been a key problem in recent years (Huijing and Ettema 1989). To address this issue Scott et al. (1996) recorded fascicle length and aponeurosis length during muscular activation of cat soleus to compare the effects of including the aponeurosis with separating it out.

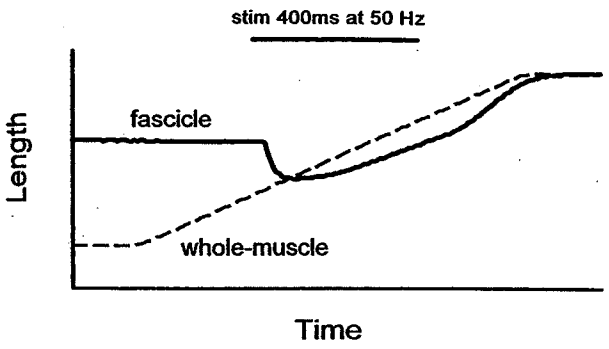

FIGURE 10.6. Simultaneous length records for fascicle and whole-muscle length during a whole-muscle stretch. When the muscle as maximally activated (indicated by solid bar above length records), the fascicles shorten even though the whole-muscle continues lengthening. (Reprinted with kind permission of Kluwer Publishers from Fig. 2a of Scott et al. 1996; © 1996 Chapman & Hall.)

A sample trial from Scott et al's (1996) study is shown in Figure 10.6 during which the length of the whole musculotendon and the length of the fascicles were recorded. While the whole musculotendon was stretched at a constant rate, when the muscle was activated the fascicles initially shortened. Because of the steep nature of the FV relationship, a model that did not separate the fascicles from the connective tissue would incorrectly predict the forces produced by the muscle during the initial stage of activation. That model would assume that the active component was stretching when in reality it was shortening, resulting in a large error for predicted force.

A second potential problem that develops if fascicle and connective tissue are not separated occurs when a model is intended to be generic. Garies et al. (1992) collected a series of FL curves for a variety of cat muscles (Figure 10.7) and used fascicle PLUS aponeurosis as the relevant length for scaling the active component. As can be seen clearly in their results, the FL curves are different for each muscle (similar results have been reported for rat muscles by Woitteiz et al. (1983)). For those of us trying to create a generic model that can describe all muscles, the conclusion from the these studies and that of Scott et al. (1996) is that the system has not been reduced enough if the aponeurosis is included with the fascicles—the fascicles and aponeuroses must be separated. In fact, the complexity of the overall system need not be increased by this reduction because

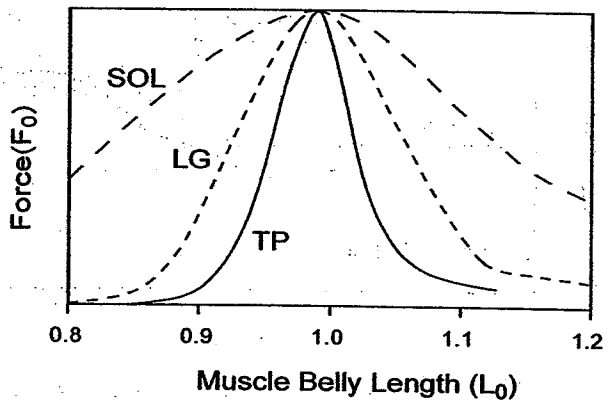

FIGURE 10.7. FL curves from three cat muscles—soleus (SOL), lateral gastrocnemius (LG) and tibialis posterior (TP). Force is normalized to maximal isometric force (F_0) and the muscle belly length at which that occurs (L_0). Muscle belly length is fascicle length PLUS aponeurosis length. (Data originally published in Baries et al. 1992.)

the aponeurosis tends to have mechanical properties that are similar to the tendon of the muscle (Scott and Loeb 1995); the two probably can be lumped into a single element in most muscles.

2.2.2 *Example B2: Separating the Active and Passive Components of the Contractile Component*

The most obvious reason for separating the active and passive components of the contractile component is that the active component scales with activation (because it is active) and the passive component does not. Unfortunately, in traditional models only part of the passive component is usually removed. The active and passive FL curves for a typical muscle are shown in Figure 10.8 as suggested by Brown et al. (1996a). PE2 is the well-known passive elasticity that can be observed simply by stretching a muscle and recording tension. PE1 is harder to observe, as it can only be seen when there is active force to counteract its action as a compression spring within the sarcomeres. PE1 exists because the myosin filament is stiff and resists compression. Normal passive shortening of a muscle to very short lengths does not reveal this phenomenon because the muscle buckles. Only by activating the muscle does PE1 become obvious.

The fact that myosin compression affects the FL curve was first suggested by Gordon et al. (1966) as an explanation for the steep portion of the ascending limb of the FL curve, but only recently has there been evidence to support it. This same evidence reveals that treating PE1 as it should be (i.e., passive) results in a simpler model. Scott et al. (1996) recorded FV curves from soleus muscle at various lengths (during maximal activation). Given our presumption of FL, FV, and F_{ACT} independence, FV curves scaled to the isometric force should all produce congruent curves. FV data (recorded at different lengths during shortening) scaled to isometric WITHOUT accounting for PE1 is shown in Figure 10.9A. The same data scaled to isometric WITH accounting for PE1 is shown in Figure 10.9B, in which the shortening half of the FV curve is indeed independent of length. A model that omitted element PE1 would actually need a considerably more complex FV component with a length-dependent term to account for these data.

A second reason for separating the active and passive FL curves is that they do not scale similarly between muscles. The active FL curve is normally scaled by L_0. Brown et al. (1996b) compared passive FL curves (PE2) from various parallel-fibered, strap-like muscles in the cat hind limb and demonstrated that different muscles have different

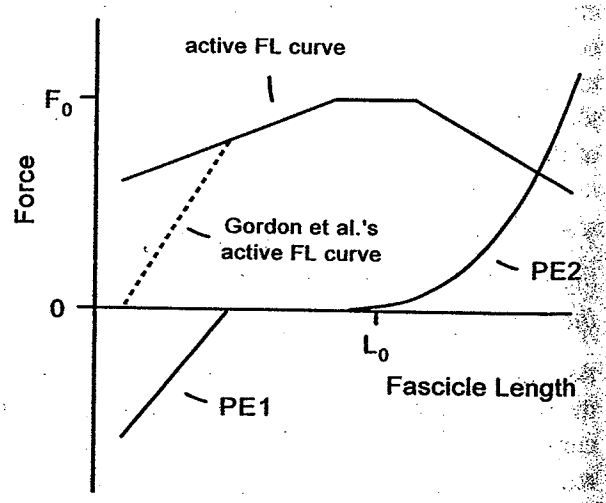

FIGURE 10.8. The shapes of the active and passive FL curves are shown here. Note the difference between Gordon et al.'s (1966) FL curve with the steep portion (dashed line) and our version (Brown et al. 1996a). The difference between the two curves is our recognition that PE1 exists as a separate component. PE1 resists compression and so produces 'negative' force. PE2 represents the well-recognized, spring-like properties the passive muscles exhibited when stretched.

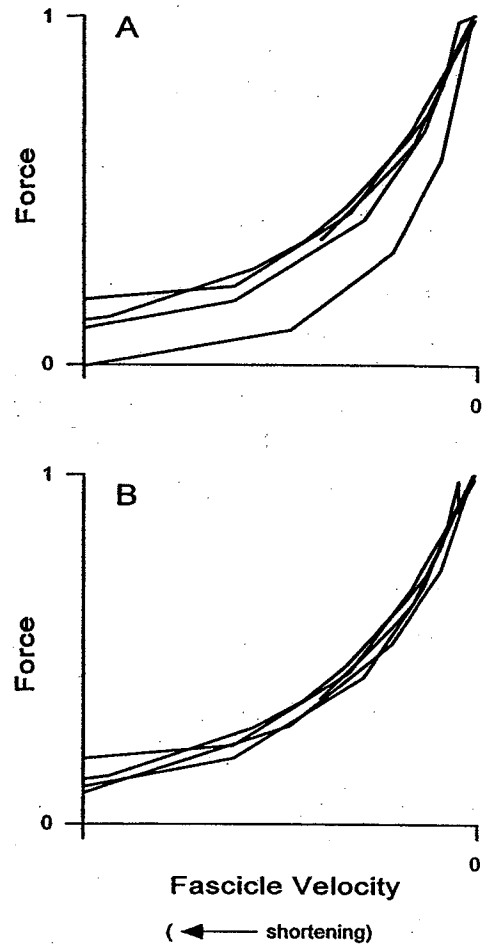

FIGURE 10.9. (A) Shortening half of FV curves from one muscle collected at different lengths without PE1 accounted for. (B) Shortening half of FV curves from one muscle collected at different lengths with PE1 accounted for—note the difference in congruity between A and B. (Data originally published in Scott et al. 1996.)

passive FL curves. The range of passive FL curves from five different muscles are shown in Figure 10.10 with all forces normalized to physiological cross-sectional area and all lengths normalized to L_0. Although there is some consistency between muscles of one type from different animals, there is a significant degree of variability between different muscles (e.g., caudofemoralis and sartorius). Treating the passive and active FL curves similarly is thus not appropriate for a generic model. Although not shown here, the conclusion of Brown et al.'s (1996b) study was that the passive FL curves (PE2) should be normalized to L_{MAX} (maximal *in situ* length of the muscle) and not L_0, consistent with the suggestion that much of PE2 arises from extrasarcomeric connective tissue rather than the myofilaments themselves.

2.2.3 *Example B3: Independence Versus Interdependence of the FL and FV Relationships*

As stated earlier, a common assumption among muscle models is the independence of the FL and FV relationships. This obviously makes the model easier to design as the two factors can be studied and modeled separately. But how realistic an assumption is it? Scott et al. (1996) designed an experiment to answer this question.

The cat soleus muscle was activated maximally over a range of velocities to produce a FV curve at a particular length. This paradigm was then repeated on the same muscle for other lengths and the resulting FV curves compared. As was shown earlier in example B2 (Figure 10.9), when the passive elements of the muscle are properly accounted for the shortening half of the FV relationship appears to be independent of length. However, the story is quite different in the lengthening half. Figure 10.11 shows the entire FV curve scaled to isometric (with the passive elements properly accounted for). Although the curves for the shortening half are congruent, the lengthening curves are not.

These results indicated that the common assumption about FL and FV independence is not entirely correct. Fortunately, these data can be described reasonably accurately by adding a length dependence to the equation describing the lengthening half of the FV curve (Brown et al. 1996a) without changing the overall form of the model. An interesting result of

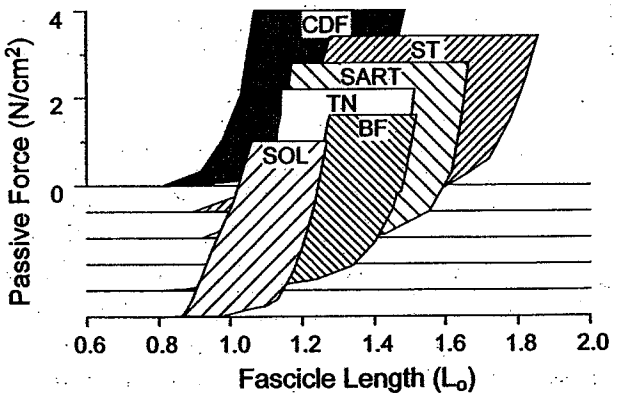

FIGURE 10.10. A large range of passive FL curves is shown from six different cat muscles. Note the large differences between muscles. N varies from 5–9 specimens for each muscle. (Reprinted with kind permission of Wiley-Liss, Inc., a subsidiary of John Wiley & Sons, Inc. from Fig. 3a of Brown et al. 1996b; © 1996 Wiley-Liss, Inc.)

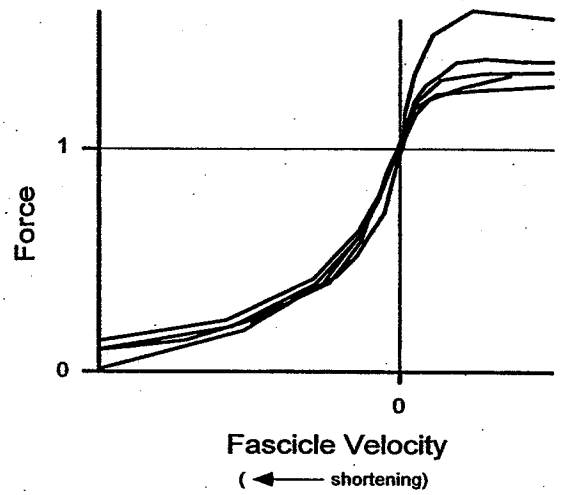

FIGURE 10.11. FV curves from one muscle collected at different fascicle lengths (from 0.67 L_0 to 1.0 L_0). Note that the shortening halves appear congruent, while there are some large differences on the lengthening half. (Data originally published in Scott et al. 1996.)

reducing the fascicle's active component into separate FL and FV components is that the observed extra length dependence upon force during active lengthening must be due to some as yet unknown property of cross-bridge dynamics—it is not simply a change in the filament overlap.

2.3 The Nervous System

The nervous system includes all neural circuitry, including both the central nervous system and the peripheral nervous system. In our models, the neural circuitry is divided into three components: Planner, Controller, and Regulator. These divisions are not based upon anatomy as was the case for both the skeletal and muscular systems, but instead are conceptual, relating to the computational properties of the circuitry and the available input–output signals at various levels of the nervous system.

We conceptualize our three divisions as follows. Planner makes the strategic decision about what is to be done (much as the general of an army does so). Controller identifies the appropriate tactics (much like a colonel or major). Regulator interprets the commands from the Controller and implements the proscribed tactics, taking local conditions into account (as a platoon commander would in the army). To provide some anatomical landmarks for the model, we might assign the premotor cortex and extrapyramidal structures to be the Planner, motor cortex as the Controller, and spinal cord as the Regulator. Models of sensorimotor control based on such divisions are under development (Loeb et al. 1990; Loeb and Brown 1995).

3 Implications for Control

So far, we have considered some of the reductionist principles that could be used to guide the development of any model. We will now build a specific model according to these principles in order to answer two specific questions about the NMS, questions that could be addressed successfully only by such a reductionist model.

3.1 Objective

The objective of the following study (presented in preliminary form by Brown et al. 1995) was to answer the following two questions:

1. Are the "complex" intrinsic properties of muscle important in responding to perturbations?
2. How does co-activation of an "overcomplete" set of muscles modify these responses?

In the first question, the reference to "complex" intrinsic properties refers to the FL and FV curves. In large systems with many muscles, simplifying muscle properties is a very good way to simplify the overall system, but leads potentially to a loss in accuracy. How do systems containing muscles with real muscle properties compare to systems containing muscles without real muscle properties?

The second question makes a reference to "overcomplete" muscles. Overcompleteness, or redundancy, refers to the observation that for any given joint, there are usually many more muscles that cross that joint than are required to achieve independent control of each degree of freedom of the joint (e.g., a one degree-of-freedom hinge joint requires two and only two muscles operating as an antagonist pair). It also refers to the fact that there are biarticular muscles (muscles that cross two joints) that have actions that appear to be redundant with respect to existing mono-articular muscles that already cross the same joints.

3.2 The Model

We chose to examine a system's response to perturbations as our representative motor task. The

model is shown pictorially in Figure 10.12A and is composed of the components listed below. Also shown in Figure 10.12A is part of a sample simulation. The task requires holding a weight in the hand (simulating a gun) with the forearm horizontal and the upper arm vertical. A perturbation (gun reaction force) is applied to the hand-held gun (circle) at the beginning of the simulation; the direction of which depends on the direction in which the gun is pointing (horizontal, 45° up or 45° down). The arm moves in response to the perturbation and the position of the hand is plotted every 10 ms. The arm position after 50 ms is shown to give a better idea graphically of what is happening. In this particular example, there is only one active muscle. The other five passive muscles are indicated by lines.

An important aspect of this model is that it is a musculoskeletal model. There is no nervous system attached. All muscle activations are held constant throughout various simulations meaning that this is a reflex-free model. The importance of this point will be made clear further on.

3.2.1 Model Components

- Three-segment robotic arm.
- Each segment is 45cm × 5cm, 2kg.
- Six massless actuators (muscles) representing the mono- and biarticular muscles found in real musculoskeletal systems (Figure 10.12B).
- Muscle lengths at 90°; joint angles defined as 90% optimal (0.9 L_0).
- Optimal isometric muscle force (F_o) of 1000N for each muscle.
- A 1kg hand-held "gun" (shown as a circle).
- Gun reaction force of 2000N lasting 10ms (equivalent to 50g bullet fired at 400 m/s).
- Second version of model includes tendons.
- Fascicle length:tendon length = 1:2.
- Moment arm decreased to one third of no-tendon version to maintain relative fascicle range of motion.
- Optimal isometric muscle force increased to 3000 N for each muscle to compensate for reduced moment arm.
- Muscle mass included (0.5 kg for monoarticulars and 1.0 kg for biarticulars; needed for mechanical stability when a velocity-sensitive actuator operates in series with a spring; He et al. 1991].

3.3 The Simulation

The details of the various simulations are listed below, with the results of the simulations shown in Figure 10.13. The response of the arm to the force perturbation was tracked for 100 ms. This time interval was chosen because it represents the time during

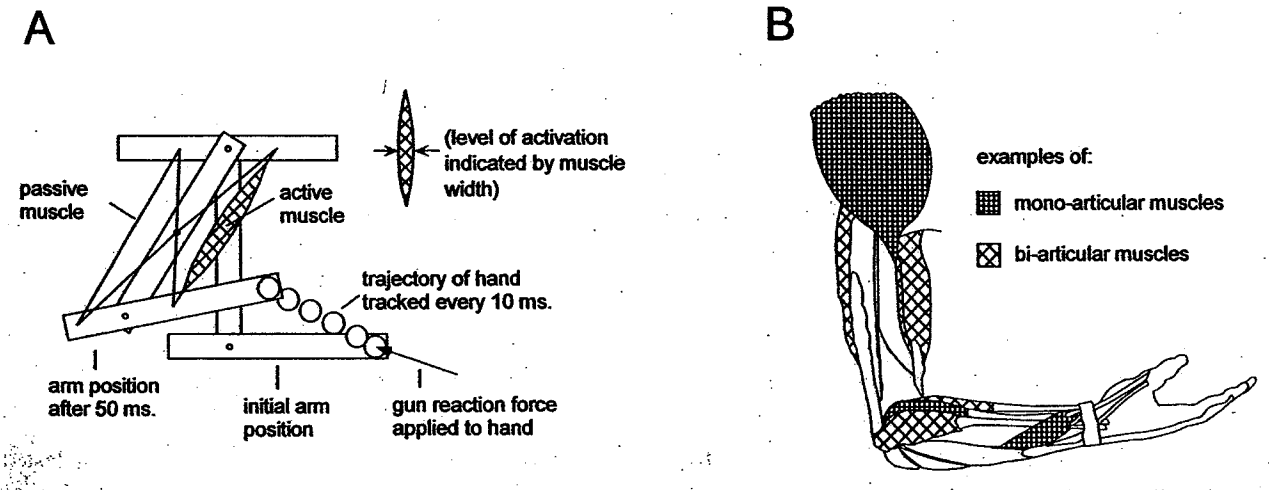

FIGURE 10.12. (A) The model is composed of three segments (two joints) and six muscles. Two of the muscles cross two joints (biarticulars) and four cross one joint (monoarticulars). Note how passive muscles are indicated with lines and active muscles with a thick muscle belly. The arms starts in the initial position with joint angles at 90°. The gun is fired which produces a gun reaction force and a kickback on the hand (circle). Only the hand is plotted as the trajectory is tracked every 10 ms. This particular simulation ends at 50 ms with the complete final arm position shown. (B) This figure shows the human arm with various mono- and biarticular muscles indicated to demonstrate their existence.

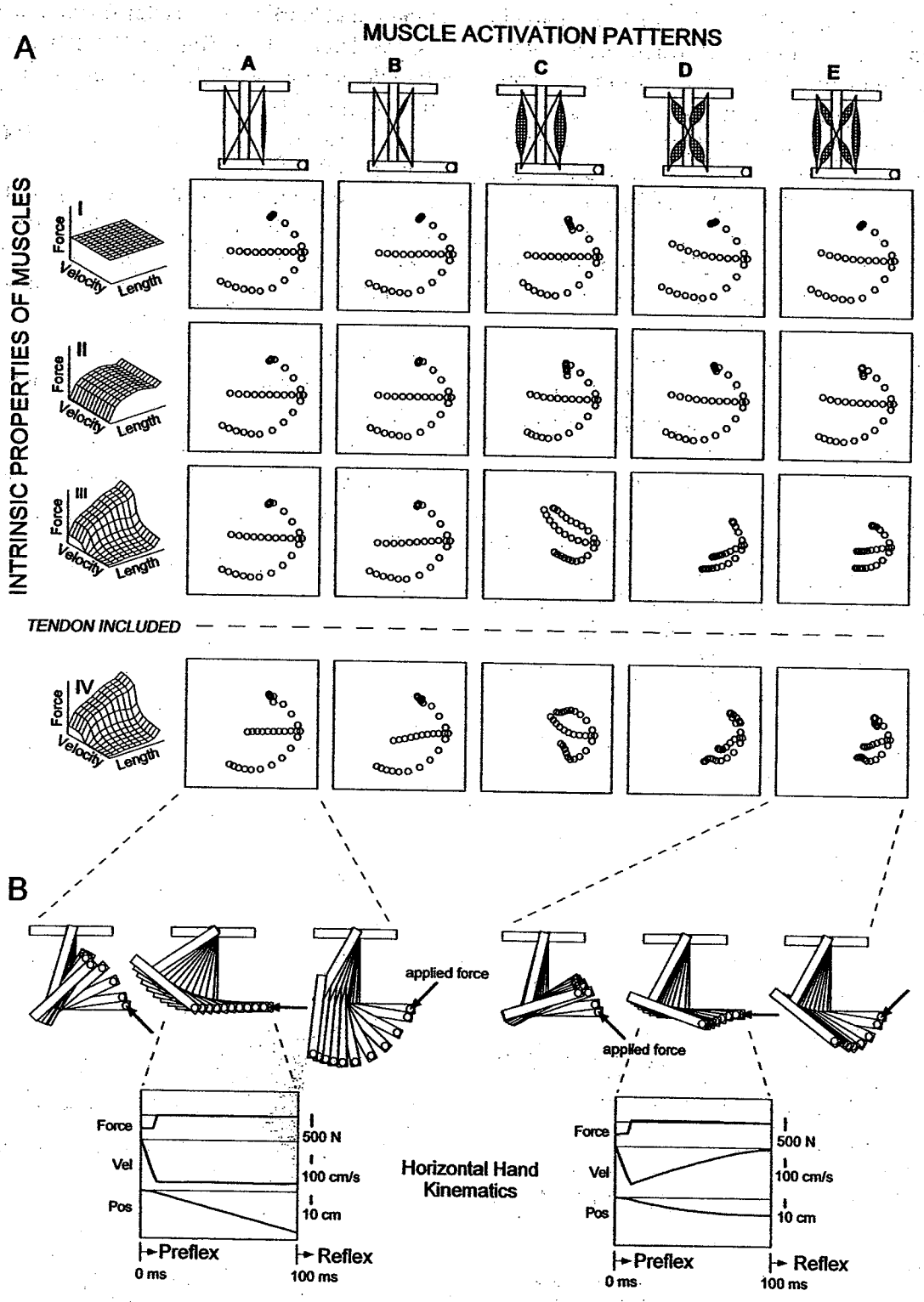

FIGURE 10.13. (A) This figure shows the results from sixty simulations. For each set of intrinsic muscle properties (I-IV) and activation patterns (A-E), three trajectories are plotted for the three different perturbation forces. To simplify the figure only the hand trajectory was plotted. The complete arm trajectories of six simulations (three from IV-A and three from IV-E are shown in part B to help clarify the figure. Each simulation lasted 100 ms with the hand plotted every 10 ms. (B) Six of the simulations from part A are shown with complete arm trajectories. The horizontal hand kinematics are shown for the simulations with the horizontal perturbation forces.

which one would expect an essentially reflex-free response (reflex loops + activation delays in human muscle ~100 ms). Three parameters were varied during various simulations: activation levels, intrinsic muscle properties and direction of perturbation.

All five activation patterns (A–E) used in the simulations were equivalent in the absence of a perturbation; the arm would remain stationary with enough net muscle torque to counteract gravity. Two of the activation patterns were equivalent 'minimal' activations: one for the biarticular flexor and one for the monoarticular flexors. The other three activation patterns used coactivation of various antagonist pairs. Each of these coactivation patterns activated the same total volume of muscle tissue.

The four sets of intrinsic muscle properties (I-IV) range from muscles with no length or velocity dependence and no tendons, to a realistic muscle with FL and FV properties plus a tendon. The one set that is not shown here but was also examined is the FV only set (no tendon). The results of that simulation were almost identical to that which had both FL and FV (no tendon).

Each of the above five activation patterns and four sets of muscle properties was examined in two ways. The first was to perturb the system with one of three different perturbations (equal magnitude, different direction) and track the response. The resulting hand trajectory is shown in Figure 10.13A with some detailed examples in Figure 10.13B. The second way in which each of these patterns and property sets was examined was by calculating the mechanical impedance at the initial position.

Mechanical impedance has three components: stiffness, viscosity, and inertia. We only calculated the stiffness and viscosity because for the majority of the simulations, there were no changes to the inertia (the lone exception being the no-tendon versus tendon version of the model). For a given stiffness measurement, the arm was displaced 1 cm from initial position in 24 evenly spaced directions. The resulting restoring forces were measured and plotted, creating the ellipses shown in Figure 10.14 (after the technique of Mussa-Ivaldi et al. (1985). Viscosity was measured in a similar manner by moving the arm through the initial position at 10 cm/s and recording the restoring force.

An important detail about the impedance measurements made on this model is that they are 100% reflex free. Although impedance tests on humans are sometimes attempted on a short enough time scale to avoid reflexes, they are often conducted over a longer time scale that results in reflex dependent impedances. Both types of impedance measurements have their virtues, but because they are different, conclusions based upon one or the other should reflect the differences inherent in the measurement technique.

3.3.1 Simulation Details

- Simulated on Working Model 3.0 with an integration time-step of 2.5 ms.
- Applied a constant level of muscle activation to counteract gravity.
- Applied a perturbation to the hand in the form of a gun reaction force.
- Tracked the resulting pre-reflex trajectory for 100 ms at 10 ms intervals.
- Five patterns of muscle activation (% activation indicated by width of muscles):
  1. Minimum biarticular (~5% activation).
  2. Minimum monoarticular (~5% activation).
  3. Biarticular coactivation (~70% activation).
  4. Monoarticular coactivation (~70% activation).
  5. Mono- and biarticular coactivation (~35% activation).
- Four sets of intrinsic properties of muscle (shown as force-length-velocity surfaces, equations and parameter values from Brown et al. 1996a):
  1. Constant force.
  2. Force-length relationship (active and passive).
  3. Force-length and force-velocity relationship (active and passive).
  4. Force-length and force-velocity relationship (active and passive)—tendon included.
- Three directions of gun reaction forces:
  1. 45° up.
  2. horizontal.
  3. 45° down.

3.4 Results and Discussion

3.4.1 Are the "Complete" Intrinsic Properties of Muscle Important in Responding to Perturbations?

The answer to this question can be seen clearly in Figure 10.13A. If we start with row I (flat intrinsic muscle properties), we see that as the level of

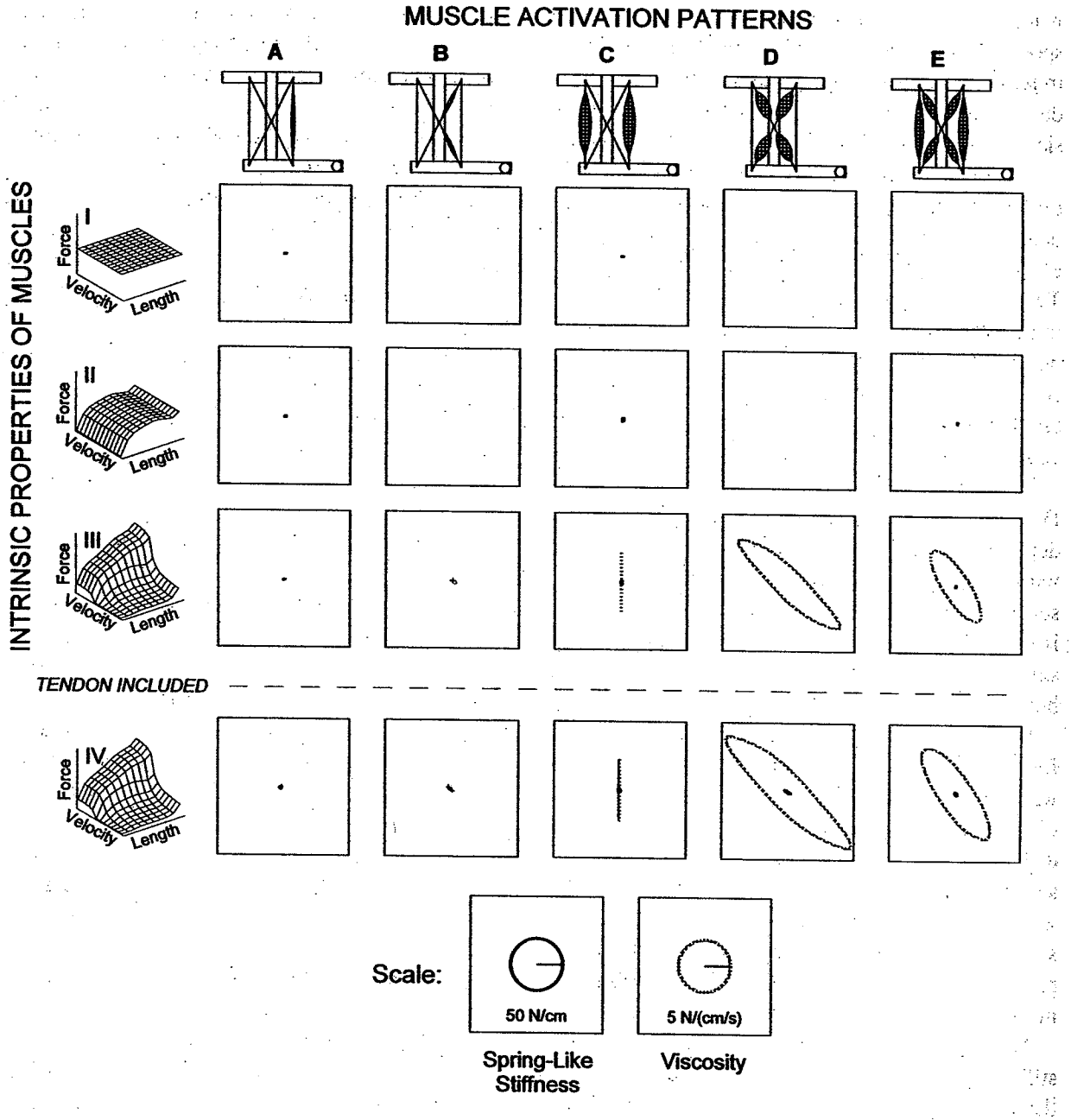

FIGURE 10.14. This figure shows the results of the impedance calculations for the four sets of intrinsic muscle properties (I-IV) and five patterns of activation (A-E). Both stiffness and viscosity ellipses are shown. For a given set of parameters, if no ellipse is shown, that is because there was an unstable (negative) impedance. The scaling factors were chosen based on the expected extreme range of displacements and velocities (estimated as a 1:10 ratio) so that the resulting ellipses indicated the relative force response expected from each component of impedance. Although not visible in this figure, the stiffness ellipses in rows III and IV had orientations parallel to those of the viscosity ellipses.

activation changes, there is no observable change in the arm's response to the perturbation. A comparison with row II (FL properties) shows that the responses are almost identical to those in row I suggesting that the FL properties of muscle provide almost no resistance to brief perturbations. We initially found this result surprising given the large amount of attention focused on the FL properties of muscle in various theories of motor control (e.g., equilibrium point hypothesis [Bizzi et al. 1992; Feldman and Levin 1995]). However, a close look at the FL curve reveals that the slopes in the regions where muscles tend to operate are not very steep.

If we look further in Figure 10.13A to row III (FL and FV properties) we finally see a change in the arm's response. As the level of activation increases above minimal, we see the arm slow and stop itself (compare the horizontal hand kinematics for IV-A and IV-E shown in Figure 10.13B). The significance of these results is that they occur in the absence of a nervous system. Row IV demonstrates that the addition of tendons and muscle masses does not significantly alter the results.

We can summarize our response to question (1) by saying that the FV properties of muscle provide a strong restoring force to perturbations, while the FL properties offer little resistance. These findings are supported by the impedance calculations (Figure 10.14) that show large viscosity impedances for rows III and IV under activation patterns C, D, and E. Note that the magnitude of the simulated impedances is of a similar magnitude to those estimated from human arm experiments (Tsuji et al. 1995). Probably the most significant aspect of these intrinsic responses is that they occur with zero time delay. Although a large perturbation such as the one in this model would likely elicit reflexes in an arm, the intrinsic properties of muscle can provide a useful response before those reflexes could effect any significant response. Because these intrinsic responses occur prereflex, we have coined the term "preflex" to describe them.

To avoid confusion, we will specifically define a preflex as: *the zero-delay, intrinsic response of a neuromusculoskeletal system to a perturbation.* Preflexes occur because of the intrinsic properties of muscle, therefore they are programmable, high-gain, and occur with zero time delay. Each and every simulation shown in Figure 10.13A has a preflex, only some of which appear to be useful for the goal of stabilizing the hand in this task (III-C, D, E and IV-C, D, E). Preflexes are not the same as reflexes nor are they a subset of reflexes.

Both preflexes and reflexes are under the control of the CNS, but via different mechanisms. The preflexes depend on the CNS's selection of a particular pattern of muscle activation to perform the nominal task from the infinitely many possible combinations created by the "overcompleteness" of the available muscles. To decide what constitutes a useful preflex, there has to be some set of expected perturbations. This set may be the Null set, in which case the gunman of our model would probably choose activation pattern A or B to conserve energy. Alternatively, if the gunman in our model wanted to fire a gun horizontally while holding it underneath a table, he would set up activation pattern D or E instead of C so that his arm would always be deflected downward in response to the firing of his gun.

Reflexes may also be programmed to deal with expected perturbations by adjusting the bias on the various interneurons that control the gain between afferent input and motor output and the bias on the unrecruited motoneurons themselves. It is common to ascribe learned responses to such reflexes, particularly when they occur over a time-course where this is feasible, but motor psychologists are beginning to appreciate the importance of preflexes under such circumstances (Almeida et al. 1995).

3.4.2 How Does Coactivation of "Overcomplete" Muscles Modify These Responses?

This question too is answered clearly in Figure 10.13A and 10.13B. Simply, the muscles appear overcomplete only when the task is underspecified. In the absence of a perturbation, all of the muscle patterns are identical in function—they hold the arm stationary, counteracting the effects of gravity. Based upon this observation, one might suggest that the muscular system is thus 'over-complete' or redundant. However, when a perturbation is applied, there are a variety of responses from the various activation patterns. Depending upon the expected set of perturbations and the desired preflex, the actual choice of activation pattern becomes well defined. In order to define a task completely, tasks must be specified in terms of the performance criteria AND the expected set of perturbations.

4 Future Directions

The model as it has been presented is still incomplete. The largest problem is the one that was least talked about in this chapter—modeling the nervous system. The lack of adequate models reflects not any lack of research in this area, but rather demonstrates the complexities found in the nervous system. Although there have been many models in the past of one portion of the nervous system or another, we

feel that future directions must account for the distinct properties and potential contributions of the various components of both the nervous system and the neuromusculoskeletal apparatus. The challenge is to create a model that is complex enough to replicate the interactive structure of the NMS system in such a way that the individual components are still recognizable and can be related to their structure and function as studied in isolation.

The model of muscle used in this study is still far from adequate to account for the full range of skeletal muscle properties that will affect the performance of NMS systems under at least some physiological conditions. This model was based on as complete a dataset as has yet been collected for the purpose of creating a model (Scott et al. 1996). Yet the dataset upon which the model was based did not describe submaximal activation, nor did it describe certain output properties that depend on activation history (e.g. yielding [Joyce, Rack, and Westbury 1969]). The muscle used in Scott et al.'s study (1996) was composed of 100% slow-twitch muscle fibers and, as yet, there is no good data-set on fast-twitch muscle fibers. The model also has no way to handle post-tetanic potentiation, which is known to occur in fast-twitch muscle fibers. Experiments are under way to collect these data so that models can be built to describe NMS systems more realistically. Until this is done, our models remain incomplete in that they describe slow-twitch muscle during maximal activation—a poor representation of most muscles and most natural activities.

Acknowledgments. This work was supported the Medical Research Council of Canada. The authors would like to thank Tiina Liinamaa for helpful comments regarding the manuscript.

References

Abraham, L.D. and Loeb, G.E. (1985). The distal hindlimb musculature of the cat. Patterns of normal use. *Exp. Brain Res.* 58:580–593.

Almeida, G.L., Hong, D., Corcos, D., and Gottlieb, G.L. (1995). Organizing principles for voluntary movement: extending single-joint rules. *J. Neurophysiol.*, 74:1374–1381.

Bizzi, E, Hogan, N., Mussa-Ivaldi, F.A., and Giszter, S. (1992). Does the nervous systgem use equilibrium-point control to guide single and multiple join movements? *Behav. Brain. Sci.*, 15:603–613.

Bonasera, S.J. and Nichols, T.R. (1996). Mechanical actions of heterogenic reflexes among ankle stabilizers and their interactions with plantarflexors of the cat hindlimb. *J. Neurosci.*, 75:2050–2055.

Brown, I.E., Scott, S.H., and Loeb, G.E. (1995). "Preflexes"—programmable, high-gain, zero-delay intrinsic responses of perturbed musculoskeletal systems. *Soc. Neurosci. Abstr.*, 21:1433 (Abstract).

Brown, I.E., Scott, S.H., and Loeb, G.E. (1996a). Mechanics of feline soleus: II. Design and validation of a mathematical model. *J. Muscle Res. Cell Motil.*, 17: 219–232.

Brown, I.E., Liinamaa, T.L., and Loeb, G.E. (1996b). Relationships between range of motion, L_o and passive force in five strap-like muscles of the feline hindlimb. *J. Morphol.*, 230:69–77.

Cavagna G.A. (1970). Elastic bounce of the body. *J. Appl. Physiol.*, 29:279–282.

Feldman, A.G. and Levin, M.F. (1995). Positional frames of reference in motor control. The origin and use. *Behav. Brain. Sci.*, 18:723–806.

Garies, H., Solomonow, M., Baratta, R., Best, R., and D'Ambrosia, R. (1992). The isometric length-force models of nine different skeletal muscles. *J. Biomech.*, 25:903–916.

Gordon, A.M., Huxley, A.F., and Julian, F.J. (1966). The variation in isometric tension with sarcomere length in vertebral muscle fibres. *J. Physiol.*, 184:170–192.

He, J., Levine, W.S., and Loeb, G.E. (1991). Feedback gains for correcting small perturbations to standing posture. *IEEE Trans. Auto. Cont.*, 36:322–332.

Huijing, P.A. and Ettema, G.T. (1989). Length-force characteristics of aponeurosis in passive muscles and during isometric and slow dynamic contractions of rat gastrocnemius muscle. *Acta. Morphol. Neerl. Scand.*, 26:51–62.

Huxley, A.F. (1957). Muscle structure and theories of contraction. *Prog. Biophys. Mol. Biol.*, 7:255–318.

Joyce, G.S., Rack, P.M.H, and Westbury, D.R. (1969). Mechanical properties of cat soleus muscle during controlled lengthening and shortening movements. *J. Physiol.*, 204:461–474.

Loeb, G.E. (1993). The distal hindlimb musculature of the cat: I. Interanimal variability of locomotor activity and cutaneous reflexes. *Exp. Brain Res.*, 96:125–140.

Loeb, G.E. and Richmond, F.J.R. (1994). Architectural features of multiarticular muscles. *Hum. Mov. Sci.*, 13:545–556.

Loeb, G.E. and Brown, I.E. (1995). Realistic neural control for real musculoskeletal tasks. *Soc. Neurosci. Abstr.*, 21:1433 (Abstr).

Loeb, G.E., Levine, W.S., and He, J. (1990). Under-

standing sensorimotor feedback through optimal control. Cold Spring Harbor Symposia on Quantitative Biology, 55:791–803.

Loeb, G.E., Pratt, C.A., Chanaud, C.M., and Richmond, F.J.R. (1987). Distribution and innervation of short, interdigitated muscle fibers in parallel-fibered muscles of the cat hindlimb. *J. Morphol.*, 191:1–15.

Mussa-Ivaldi, F.A., Hogan, N., and Bizzi, E. (1985). Neural, mechanical, and geometric factors subserving arm posture in humans. *J. Neurosci.*, 5:2732–2743.

Scott, S.H. and Loeb, G.E. (1995). The mechanical properties of the aponeurosis and tendon of the cat soleus muscle during whole-muscle isometric contractions. *J. Morphol.*, 224:73–86.

Scott, S.H., Brown, I.E., and Loeb, G.E. (1996). Mechanics of feline soleus: I. Effect of fascicle length and velocity on force output. *J. Muscle Res. Cell Motil.*, 17:205–218.

Tsuji, T., Morasso, P.G., Goto, K., and Ito, K. (1995). Human hand impedance characteristics during maintained posture. *Biol. Cybern.*, 72:475–485.

Woittiez, R.D., Huijing, P.A., and Rosendal, R.H. (1983). Influence of muscle architecture on the length-force diagram of mammalian muscle. *Pflugers Arch.*, 399:275–279.

Young, R.P., Scott, S.H., and Loeb, G.E. (1993). The distal hindlimb musculature of the cat: II. Multiaxis moment arms of the ankle joint. *Exp. Brain Res.*, 96:141–151.

Zajac, F.E. and Gordon, M.E. (1989). Determining muscle's force and action in multi-articular movement. *Exerc. Sport Sci. Rev.*, 17:187–230.